Current Topics in Biophysics 2005, 29(1-2), 101-107

NONINVASIVE IMAGING OF OXYGENATION IN A TRANSPLANTED TUMOR

ANNA BRATASZ, PERIANNAN KUPPUSAMY

Center for Biomedical EPR Spectroscopy and Imaging, Davis Heart and Lung Research Institute, Department of Internal Medicine, The Ohio State University, Columbus, USA

Electron paramagnetic resonance (EPR) spectroscopy, utilizing particulate oximetry probes, was used to perform repeated measurement and imaging of pO_2 in a transplanted tumor model. The probes were permanently embedded in the tumor for injection into mice by pre-internalization or co-implantation of RIF-1 (radiation-induced fibrosarcoma) cancer cells. This procedure enabled repeated measurements of the oxygen concentration in the tumor for more than 2 weeks during its growth phase. The particulates were stable and nontoxic to the tumor cells. An *in vitro* cellular membrane integrity assay showed no apparent effect on membrane permeability after 24-hour co-incubation of RIF-1 cells with the oxygen probe. However, *in vivo* tumor growth showed a decrease in tumor growth rate. The measurements indicated that the pO_2 of the tumor decreased rapidly with tumor growth in the model of co-implanted oxygen probe. However, the oxygen level was very low from the beginning of tumor development in the internalized model. EPR imaging revealed a non-uniform distribution of the embedded particulates in the tumor. Oxygen mapping of the tumor, obtained by spectroscopic EPR imaging, showed a significant variation of pO_2 within the tumor. In summary, EPR spectroscopy and imaging, using an embedded oximetry probe, enabled accurate and repeated measurements of pO_2 in growing tumors under non-perturbing conditions.

INTRODUCTION

Tumors, in general, are poorly oxygenated compared to host tissue. The oxygen deficiency, known as hypoxia, is associated with increased resistance of the tumor cells to chemotherapy or radiation (Hockel & Vaupel, 2001; Vaupel, Kelleher & Hockel, 2001). Tumor oxygenation is strongly correlated with the treatment outcome of chemo- or radiotherapy in several human tumors (Hockel, Knoop, Schlenger, Vorndran, Baussmann, Mitze, Knapstein & Vaupel, 1993; Okunieff, Hoeckel, Dunphy, Schlenger, Knoop & Vaupel, 1993). Another confounding factor that may potentially interfere with the prediction of the treatment outcome is the non-uniform distribution of oxygenation within the same tumor (Brurberg, Graff & Rofstad, 2003; Evans, Hahn, Magarelli & Koch, 2001; Hunjan, Zhao, Constantinescu, Hahn, Antich & Mason, 2001). Many tumors are characterized with regions (pockets) of hypoxia, even in well-oxygenated tissue. Thus, information on the magnitude and distribution of tumor oxygenation and its variations as a function of tumor size, response to therapeutic stress (e.g., radiation), and preconditioning (e.g., hyperoxic treatment) would be valuable to help understand and develop effective treatment strategies for targeted cancer-cell killing. This information would require the availability of tools and procedures capable of repetitive, noninvasive imaging of oxygen concentration in living tissues.

Of the variety of methods that are available for tissue oximetry (Stone, Brown, Phillips & Sutherland, 1993), the magnetic resonance-based methods, such as MRI, electron paramagnetic resonance (EPR) spectroscopy, and imaging (EPRI), have the advantage of noninvasive imaging of the oxygen concentration in tissues (Dunn, O'Hara, Zaim-Wadghiri, Lei, Meyerand, Grinberg, Hou, Hoopes, Demidenko & Swartz, 2002; Fan, River, Zamora, Al-Hallaq & Karczmar, 2002; Krishna, English, Yamada, Yoo, Murugesan, Devasahayam, Cook, Golman, Ardenkjaer-Larsen, Subramanian & Mitchell, 2002; Mason, Hunjan, Le, Constantinescu, Barker, Wong, Peschke, Hahn & Antich, 1998). The EPR-based method, known as "EPR oximetry", uses spin probes whose EPR lines are broadened by molecular oxygen. The oxygen-induced line-broadening is usually linear with respect to the partial pressure of oxygen (pO_2), hence the measured line-width can be converted to oxygen concentration using appropriate standard curves. The measurements can be performed noninvasively and repeatedly over periods of months at the same site. This approach uses implants of particulate oximetry probes such as lithium phthalocyanine (LiPc), and lithium octa-n-butoxynaphthalocyanine (LiNc-BuO) whose EPR line-widths are highly sensitive to local oxygen

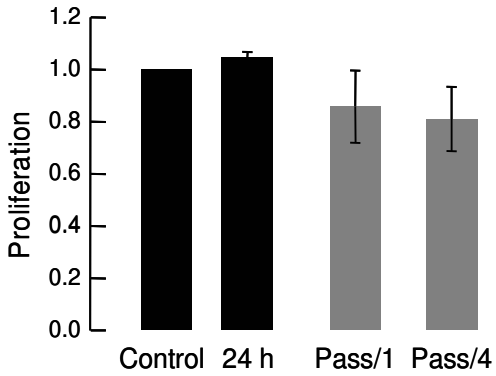

Fig. 1. Effect of the oximetry particulates on the cellular membrane integrity and proliferation of RIF-1 cells. Cells were cultured in the presence of extra-cellular LiPc crystals (size: 20 – 26 μm) for 24 h or intracellular LiNc-BuO crystals (size < 1 μm) assayed at the end of a single or 4 passages. The results indicate that the particulates had no significant effect on the viability of RIF-1 cells.

concentration (Ilangovan, Li, Zweier, Krishna, Mitchell & Kuppusamy, 2002; Pandian, Parinandi, Ilangovan, Zweier & Kuppusamy, 2003). These probes are stable in tissues, nontoxic, and biocompatible. They can be implanted at the desired site or, with a suitable coating, they can be infused into the vasculature for targeted delivery to tissues (Ilangovan, Bratasz, Li, Schmalbrock, Zweier & Kuppusamy, 2004). In addition, these probes can be internalized in cells enabling highly accurate measurement of intracellular pO_2 (Pandian *et al*., 2003).

We report new approaches for noninvasive and repeated determination of oxygen concentration in experimental tumors by EPR-based oximetry using embedded paramagnetic particulates. Unlike the existing methods of oxygen measurement, wherein the probes (needle electrodes, optical probes, or EPR implants) are physically inserted during measurement, the new approach used probes that were permanently embedded in the tumor. A particular advantage of this procedure was that it was noninvasive, both in terms of implantation of the probe, as well as in obtaining readouts of oxygen. Further, EPR imaging measurements could be performed to map the spatial distribution of oxygen concentration in the tumor.

MATERIALS AND METHODS

Reagents

Cell culture medium (RPMI 1640), fetal bovine serum, penicillin/streptomycin, sodium pyruvate, trypsin, and phosphate-buffered saline (PBS) were purchased from Gibco BRL (Grand Island, NY). The in vitro MTT Toxicology Assay Kit was obtained from Sigma (St. Louis, MO). Lithium phthalocyanine (LiPc) and lithium octa-n-butoxynaphthalocyanine (LiNc-BuO) probes were synthesized as reported (Ilangovan *et al*., 2002; Pandian *et al*., 2003).

Mice

Female C3H mice were obtained from Frederick Cancer Research Center Animal Production (Frederick, MD). The animals were housed five per cage in a climate- and light-controlled room. Food and water were allowed *ad libitum*. The animals were 50-days old and weighed about 25 g at the time of the experiment. Animals were anesthetized with ketamine and xylazine (i.p.). The animals inhaled either room air (21% O_2) or carbogen (mixture of 95% O_2 and 5% CO_2) through a nose cone. During the measurements, the body temperature of the animal was maintained at 37±1 ^oC by an infra-red lamp placed just above the animal. The body temperature was monitored using a rectal thermistor probe.

Tumor growth and implantation of the oxygen probe

Radiation-induced fibrosarcoma-1 (RIF-1) cancer cells were used in the present study. The cells were grown in RPMI-1640 medium supplemented with 10 % fetal bovine serum and 1 % penicillin/streptomycin in an atmosphere of 95 % air and 5 % CO_2 at 37°C. Cells were trypsinized, centrifuged and suspended in PBS (without calcium and magnesium ions). The oxygen-sensing probes were introduced into the tumor in two different ways. (i) Co-implantation: A suspension of $1x10^6$ RIF-1 cells mixed with 20 μg of LiPc in 0.06 ml of PBS was injected into the upper portion of the right hind limb of mice. (ii) Intracellular internalization: Cells were cultured in 75 cm^2 dishes for 4 passages, together with particulates of LiNc-BuO (size < 1 μm). Then the cells were washed 4 times (to remove the extracellular particulates), trypsinized, centrifuged, and suspended in PBS. The uptake of the particulates into the cells was quantified by EPR spectroscopy. The cells (1×10^6), internalized with the particulates, were injected into the upper portion of the right hind limb of C3H mice and grown as solid tumor.

EPR oximetry and imaging

Microcrystals of lithium phthalocyanine (LiPc) or lithium octa-*n*-butoxynaphthalocyanine (LiNc-BuO) were used as probes for EPR oximetry. The peak-to-peak line-width of the EPR spectra of the

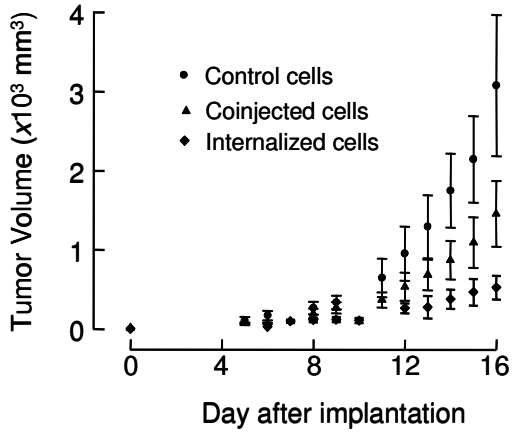

Fig. 2. Effect of the oximetry particulates on the growth of RIF-1 tumor. Tumor growth volume curves are shown for tumors without probe (control), with cells co-implanted with LiPc, and with cells internalized with LiNc-BuO particulates. The tumor volume was obtained from the 3 orthogonal diameters of the tumor. The tumors, in general, showed exponential growth rates. However, the data from co-implanted and internalized groups showed significantly reduced growth compared to those from the control group.

probes showed a linear relationship with pO_2. The value of pO_2 in tissue was obtained from a standard curve of the EPR line-width versus the oxygen concentration as reported previously (Ilangovan *et al.*, 2002). The EPR measurements were performed by using an L-band (1.2 GHz) EPR spectrometer with a surface coil resonator.

Cell proliferation assay

Cells were plated into 96-well dishes at a density of 5×10^4 cells per well containing 100 µl RPMI-1640 (without phenol red and supplemented with 10% fetal bovine serum and 1% penicillin/streptomycin), incubated in an atmosphere of 95% air / 5% CO_2 at 37°C for 12h, then assayed for cell proliferation using an MTT-based Toxicology Assay Kit. Measurements were taken using a Beckman Coulter AD 340 UV-VIS spectrophotometer set at a wavelength of 570 nm with a reference filter at 690 nm. The data were obtained as an average of 3-5 wells.

Cellular membrane integrity assay

The toxic effect of the crystals on RIF-1 cells was studied by a cellular membrane integrity assay. Cells were grown in 60-mm Petri dishes containing RPMI-1640 supplemented with 10% FBS and 1% penicillin/streptomycin. When the cells reached 60% confluence, 1 mg of LiPc was added to 4 ml of culture medium. The cells were incubated for 24 h, and then rinsed 5 times with PBS to remove the particulates. The cells were trypsinized, centrifuged, and stained with 1% trypan blue to assay the integrity of the cell membrane.

Statistical analysis

Data are expressed as Mean±SEM. Comparisons among groups were performed by student's t-test. The significance level was set at $p<0.05$.

RESULTS

Effect of particulates on cells and tumor growth

The cytotoxicity of particulates of LiPc and LiNc-BuO on the RIF-1 cells was studied by a cellular membrane integrity assay using trypan blue. The RIF-1 cells, at 60% confluence in 60-mm culture dishes, were co-incubated with the particulates for 24 h and then assayed for cytotoxicity. The results showed that the particulates did not exert any significant effect on the membrane integrity of the treated cells when compared to that of the untreated cells (Figure 1). Since the sizes of these needle-shaped particulates were in the range of 60-80 µm, they were expected to remain primarily outside of the cells. In another set of experiments, the influence of nanocrystalline particulates of LiNc-BuO on cell proliferation was studied using an MTT assay. After 4 cycles of passages, the cells for both the untreated controls and those treated with LiNc-BuO particulates were washed with PBS to remove the externally attached particulates and then trypsinized. The internalization of the particulates in the cells was confirmed by EPR. About 50,000 of these cells (per well) were then plated in 96-well dishes. After overnight incubation, the cells were subjected to the MTT assay. As seen in Figure 1, the growth rate of these cells containing the LiNc-BuO particulates was slightly lower.

The effect of the particulates on the growth rate of the RIF-1 tumor was studied by using a tumor growth volume curve. All three sets of tumors (untreated control, LiPc-co-implanted, and LiNc-BuO-internalized) showed exponential growth rates. However, the co-implanted and internalized groups showed significantly reduced growth volume curves compared to the control group (Figure 2).

Change of pO_2 as a function of tumor growth

RIF-1 cells, either mixed with LiPc or internalized with LiNc-BuO particulates, were injected in the hind limbs of mice, as described in the methods section. The extra- and intra-cellular pO_2 values

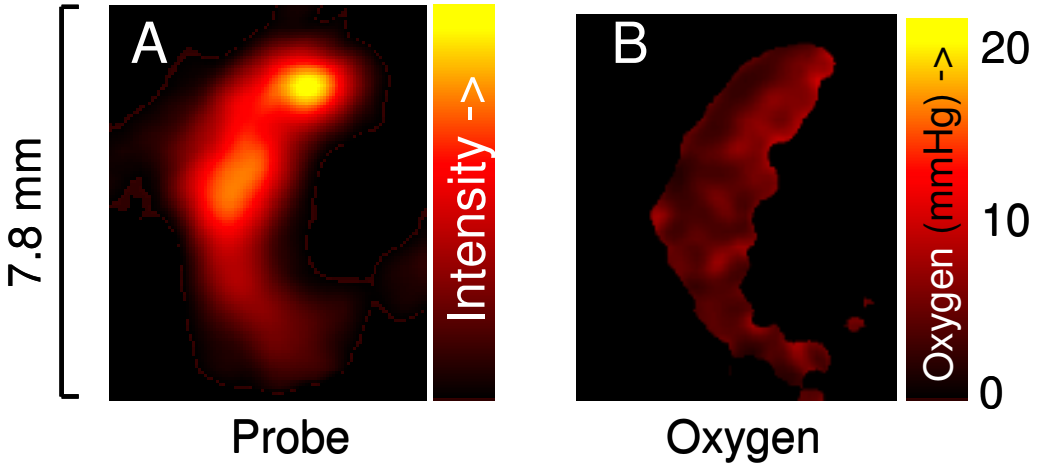

Fig. 3. Representative images of embedded particulates of LiPc and oxygen in a RIF-1 tumor. The images were obtained on day 11 after inoculation of a mouse with a mixture of RIF-1 cells and LiPc. A: Spatial image showing the distribution of the particulates in the tumor. B: Oxygen image, obtained from spectroscopic imaging, of the tumor in a mouse breathing room air. Note that the oxygen information was obtained only from the regions where the particulates were present. The oxygen image shows the presence of hypoxic regions in the tumor.

within the growing tumor were measured by EPR spectroscopy daily for 2 weeks after injection of the cells. The pO_2 value in the tissue with co-implanted probe (extra-cellular pO_2) was 13 ± 2 mmHg on day 1 and decreased to about 4 mmHg on day 9. On the other hand, the intracellular pO_2 levels in the case of internalized particles remained almost the same (around 2-3 mmHg) during the whole period of tumor growth.

Mapping of oxygen concentration in growing tumor

EPR imaging was used to determine the distribution of the co-implanted or internalized particulates in the solid tumor. It was observed, in the co-implanted model, that the particulates were confined to a small region (about 5×5×8 mm^3 in a tumor of about 10×12×12 mm^3 size), which is 15% of the tumor volume (Figure 3). We further performed spectral-spatial (spectroscopic) EPR imaging on the same animals, at the same time, to map the distribution of the oxygen concentration in the tumor. This technique used oxygen-dependent lineshape information from the collected projections to obtain pO_2 values at each voxel in the image of the particulates. Figure 4, from tumor with internalized particles, shows the oxygen maps obtained at two different time points of tumor development, namely the 5^{th} and 9^{th} day, after inoculation. Figure 4 also shows the frequency plot (number of occurrences of a particular tumor pO_2 value in imaged region). The mean and median pO_2 values of the tumor on day 5 were 9.07 mmHg and 7.84 mmHg, respectively. On day 9, the mean and median pO_2 values changed to 7.40 mmHg and 5.02 mmHg, respectively. The data suggests a substantial decrease in the tumor pO_2 during the growth period. This is also evident from the left-shift of the values on day 9 (skew: 1.25) as compared to the distribution on day 5 (skew: 0.63).

DISCUSSION

The present study demonstrated a new approach for the monitoring of variations in the oxygen concentration in growing tumors by EPR oximetry using embedded paramagnetic particulates. A particular advantage of the new method was that it was noninvasive, both in terms of implantation of the probe as well as in obtaining readouts of oxygen concentrations. This was in contrast to most other methods of oxygen measurement that require the infusion of an oxygen-sensor or insertion of a needle, catheter, or probe-head into the desired location resulting in injury to the tissue and leading to artifacts in the measured pO_2 values. In addition, the new method avoided the problems associated with the recurrence of the invasive procedure for repetitive measurements of oxygen over a period of time extending days to weeks. The invasive methods generate two types of errors: (i) the measurements are often performed from a freshly injured site, wherein trauma associated with the injury, i.e. disruption of capillary blood vessels and inflammation processes at the measurement site, may lead to erroneous values of oxygen levels and (ii) repeated measurements do not allow the placement of the probe exactly at the same location each time. The present method, in addition to overcoming the

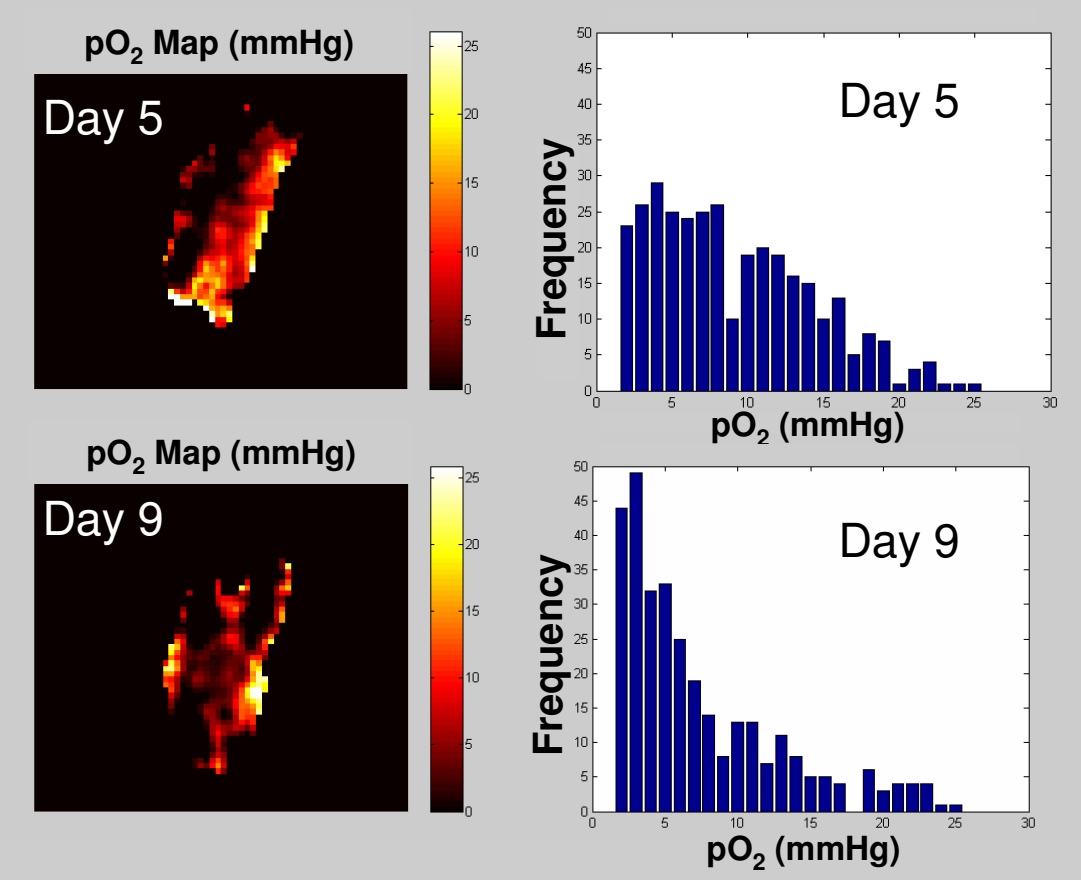

Fig. 4. Oxygen mapping in a RIF-1 tumor obtained on day 5 and day 9 of tumor growth. Images were obtained by spectral-spatial (spectroscopic) EPR imaging using an L-band (1.32 GHz) EPR spectrometer. The frequency of oxygen level in tumor tissue is shown in the right panels. Significant changes in the magnitude and distribution of oxygen are seen in the tumor on day 9. The spread in the frequency plot on day 9 is narrowed down with a shift to lower pO_2 values (median pO_2, 5.02 mmHg) as compared to the data on day 5 (median pO_2, 7.40 mmHg).

above limitations, also enabled accurate determination of oxygen concentration in the tumor.

We have previously measured the pO_2 values in RIF-1 tumor by implanting the LiPc probe directly into the tumor when the tumor was approximately 6 mm in diameter and found that the tumor was significantly hypoxic and continued to be hypoxic thereafter, during the growth of the tumor (Ilangovan *et al*., 2002). The present study using LiPc co-implanted with the tumor cells enabled us to monitor the changes in the tissue oxygenation that occurred immediately after inoculation. It was observed that the pO_2 rapidly decreased from the normal tissue value of 14 ± 2 mmHg to about 4 mmHg within 6 days when the tumor volume was just ~75 mm^3 (corresponding to ~4 mm in diameter). Thus, it appeared that tissue oxygenation fell off rapidly in the very early stages of the solid tumor formation. This suggested that tumor hypoxia occurred very early in the tumor progression due to the insufficient supply of oxygen to the exponentially proliferating cells.

The pO_2 values measured as a function of tumor growth using EPR oximetry showed some striking similarities to the results previously reported using other methods. For example, Mason *et al*. (Mason, Antich, Babcock, Constantinescu, Peschke & Hahn, 1994) used the ^{19}F nuclear magnetic resonance spin relaxation rate of a perfluorocarbon (PFC) emulsion to measure the pO_2 value in a Dunning prostate rat tumor R3327-AT1. They reported a pO_2 value of 75 mmHg in a small tumor (~10 mm). The pO_2, however, dropped to ~1 mmHg in the core when the tumor size had doubled. Baldwin and Ng (1996) measured the pO_2 in individual KHT murine sarcomas using PFC emulsion and magnetic resonance spectroscopy/ imaging. The median pO_2 of the tumor decreased from 60 mmHg to 0 mmHg corresponding to tumor masses of 0.2 g to 1.8 g, respectively. Although the overall trend in the change of pO_2 as a function of tumor growth in the RIF-1 tumor is similar to that of the tumors reported, the absolute magnitudes of the values are clearly different. The differences in

the observed levels of pO_2 can be attributed to the method used. The EPR method measures the partial pressure of oxygen in the tumor, while the MRI method detects the concentration of dissolved oxygen in the tissue. Although the studies used different types of experimental tumors, a rapid decrease of pO_2 in the tumor to an almost anoxic level during tumor growth, is a striking feature that is, nevertheless, common to both the MRI and EPRI methods.

The frequency plot of tumor oxygenation obtained in the present work showed a wide-spread heterogeneity in the pO_2 values. Similar distribution of pO_2 values were observed with the use of polarographic electrodes (Adam, Dorie & Brown, 1999). This frequency plot was different from the histogram normally obtained from the polarographic electrode measurements where the polarographic electrode was physically inserted into different locations. Here the values were obtained from the individual pixels in the image. Thus in a 125×125 pixel image, as in the present case, the values were read at 125×125 points within the sampling area of 5 mm^2. Such a high-resolution pO_2 map was only possible with imaging techniques. Usually large scatters are observed in the polarographic electrodes which are attributed to the inaccuracy of the measurement and values pooled from different animals. In the present approach, the same animals were used for pO_2 measurements throughout the period of interest so that the measurements were expected to be more consistent.

In general, the intracellular pO_2 levels were very low from the beginning of tumor growth and stayed almost at the same level during the 2 weeks of measured tumor growth. The spread of the pO_2 values in the frequency plot was an indication of the heterogeneity of the oxygen concentration in the tumor. As observed in the present study, there was considerable heterogeneity in the distribution of oxygen in the RIF-1 tumor. It was also noteworthy that the spread in the frequency plot on day 9 was narrowed down with a shift to lower pO_2 values as compared to the data on day 5.

SUMMARY AND CONCLUSIONS

In the present study we have demonstrated and established a novel procedure to obtain pO_2 data, noninvasively and repeatedly, from a growing tumor using EPR oximetry. The method used co-implantation of microcrystalline oximetry probes with the tumor cells. The probe particulates were embedded (intra-cellular or extra-cellular) in the tumor, thus enabling very accurate and reliable measurements of pO_2 without causing any perturbation to the tissue during the measurements. The measurements were performed in growing RIF-1 tumors in the subcutaneous tissue of a hind leg of C3H mice. The results showed that while the extracellular pO_2 decreased very sharply during the first few days of implantation and reached ~4 mmHg, the intracellular pO_2 levels in the case of internalized cells remained almost the same (around 2-3 mmHg) during the 2 weeks of measured tumor growth. Spatial mapping of the probe particulates showed that the probes were distributed heterogeneously, but within a region of the growing tumor. The imaging also enabled the mapping of oxygen concentration in the region of the probe distribution within the tumor. The pO_2 values in the tumor showed significant hypoxia and heterogeneity in the tumor volume. In summary, the *in vivo* measurement and imaging using an embedded oximetry probe enabled noninvasive visualization of changes in oxygen concentration during the growth of implanted RIF-1 tumor in mice.

Acknowledgement

We thank Drs. G. Ilangovan and R. P. Pandian for their help with the probe and EPR measurements. We also thank Nancy Trigg for critical reading of the manuscript. We acknowledge the financial support from the NIH grants CA 78886 and EB004031.

REFFERENCES

Adam M. F., Dorie M. J. & Brown J. M., (1999). Oxygen tension measurements of tumors growing in mice. *Int J. Radiat. Oncol. Biol. Phys.*, **45,** 171-180.

Baldwin N. J. & Ng T. C., (1996). Oxygenation and metabolic status of KHT tumors as measured simultaneously by 19F magnetic resonance imaging and 31P magnetic resonance spectroscopy. *Magn. Reson. Imaging*, **14,** 541-551.

Brurberg K. G., Graff B. A. & Rofstad E. K., (2003). Temporal heterogeneity in oxygen tension in human melanoma xenografts. *Br. J. Cancer*, **89,** 350-356.

Dunn J. F., O'Hara J. A., Zaim-Wadghiri Y., Lei H., Meyerand M. E., Grinberg O. Y., Hou H., Hoopes P. J., Demidenko E. & Swartz H. M., (2002). Changes in oxygenation of intracranial tumors with carbogen: a BOLD MRI and EPR oximetry study. *J. Magn. Reson. Imaging*, **16,** 511-521.

Evans S. M., Hahn S. M., Magarelli D. P. & Koch C. J., (2001). Hypoxic heterogeneity in human tumors: EF5 binding, vasculature, necrosis, and proliferation. *Am. J. Clin. Oncol.*, **24,** 467-472.

Fan X., River J. N., Zamora M., Al-Hallaq H. A. & Karczmar G. S., (2002). Effect of carbogen on tumor

oxygenation: combined fluorine-19 and proton MRI measurements. *Int. J. Radiat. Oncol. Biol. Phys.*, **54,** 1202-1209.

Hockel M., Knoop C., Schlenger K., Vorndran B., Baussmann E., Mitze M., Knapstein P. G. & Vaupel P., (1993). Intratumoral pO2 predicts survival in advanced cancer of the uterine cervix. *Radiother. Oncol*, **26,** 45-50.

Hockel M. & Vaupel P., (2001). Tumor hypoxia: definitions and current clinical, biologic, and molecular aspects. *J. Natl. Cancer Inst.*, **93,** 266-276.

Hunjan S., Zhao D., Constantinescu A., Hahn E. W., Antich P. P. & Mason R. P., (2001). Tumor oximetry: demonstration of an enhanced dynamic mapping procedure using fluorine-19 echo planar magnetic resonance imaging in the Dunning prostate R3327-AT1 rat tumor. *Int. J. Radiat. Oncol. Biol. Phys.*, **49,** 1097-1108.

Ilangovan G., Bratasz A., Li H., Schmalbrock P., Zweier J. L. & Kuppusamy P., (2004). In vivo measurement and imaging of tumor oxygenation using coembedded paramagnetic particulates. *Magn. Reson. Med.*, **52,** 650-657.

Ilangovan G., Li H., Zweier J. L., Krishna M. C., Mitchell J. B. & Kuppusamy P., (2002). In vivo measurement of regional oxygenation and imaging of redox status in RIF-1 murine tumor: effect of carbogen-breathing. *Magn. Reson. Med.*, **48,** 723-730.

Krishna M. C., English S., Yamada K., Yoo J., Murugesan R., Devasahayam N., Cook J. A., Golman K., Ardenkjaer-Larsen J. H., Subramanian S. & Mitchell J. B., (2002). Overhauser enhanced magnetic resonance imaging for tumor oximetry: coregistration of tumor anatomy and tissue oxygen concentration. *Proc. Natl. Acad. Sci. U.S.A.*, **99,** 2216-2221.

Mason R. P., Antich P. P., Babcock E. E., Constantinescu A., Peschke P. & Hahn E. W., (1994). Noninvasive determination of tumor oxygen tension and local variation with growth. *Int. J. Radiat. Oncol. Biol. Phys.*, **29,** 95-103.

Mason R. P., Hunjan S., Le D., Constantinescu A., Barker B. R., Wong P. S., Peschke P., Hahn E. W. & Antich P. P., (1998). Regional tumor oxygen tension: fluorine echo planar imaging of hexafluorobenzene reveals heterogeneity of dynamics. *Int. J. Radiat. Oncol. Biol. Phys.*, **42,** 747-750.

Okunieff P., Hoeckel M., Dunphy E. P., Schlenger K., Knoop C. & Vaupel P., (1993). Oxygen tension distributions are sufficient to explain the local response of human breast tumors treated with radiation alone. *Int J. Radiat. Oncol. Biol. Phys.*, **26,** 631-636.

Pandian R. P., Parinandi N. L., Ilangovan G., Zweier J. L. & Kuppusamy P., (2003). Novel particulate spin probe for targeted determination of oxygen in cells and tissues. *Free Radic. Biol. Med.*, **35,** 1138-1148.

Stone H. B., Brown J. M., Phillips T. L. & Sutherland R. M., (1993). Oxygen in human tumors: correlations between methods of measurement and response to therapy. Summary of a workshop held November 19-20, 1992, at the National Cancer Institute, Bethesda, Maryland. *Radiat. Res.*, **136,** 422-434.

Vaupel P., Kelleher D. K. & Hockel M., (2001). Oxygen status of malignant tumors: pathogenesis of hypoxia and significance for tumor therapy. *Semin. Oncol.*, **28,** 29-35.